Journal of Computational Physics 228 (2009) 3851–3857

Contents lists available at ScienceDirect

Journal of Computational Physics

journal homepage: www.elsevier.com/locate/jcp

A Monte Carlo model for seeded atomic flows in the transition regime

S. Longo [a,b,*], P. Diomede [a]

[a] Dipartimento di Chimica dell'Universita' di Bari, Via Orabona 4, 70126 Bari, Italy
[b] CNR-IMIP Bari, via Amendola 122/D, 70125 Bari, Italy

ARTICLE INFO

Article history:
Received 24 June 2008
Received in revised form 23 December 2008
Accepted 14 February 2009
Available online 26 February 2009

Keywords:
Multi-component flows
Compressible flows
Rarefied flows
Monte Carlo simulation
Numerical methods

ABSTRACT

A simple model for the numerical determination of separation effects in seeded atomic gas flows is presented. The model is based on the known possibility to provide a statistically convergent estimate of the exact solution for a linear transport equation using the test particle Monte Carlo method. Accordingly, the flow field of the main gas is preliminary calculated and as a second step the linear transport equations obtained by fixing the target distribution in the collision term of the Boltzmann equation for both main and minority components are solved. Both solutions are based on appropriately devised test particle Monte Carlo methods. The second step, the critical one in evaluating the separation effects, is exact and thereby completely free of numerical diffusion. The model is described in details and illustrated by 2D test cases of atomic separation in shock fronts.

1. Introduction

Seeded gas flows are flows where a main, or carrier component is mixed with one or more impurities or seeds with a small mole fraction. They occur frequently in chemistry, physics and their applications. Often the majority component is an atomic gas. An example is the use of molecular flows of atomic gas where seed particles are test species to be studied by spectroscopic means after the adiabatic expansion cools the gas down to very low temperatures [1]. Another example is in the technology of negative ions sources to be used in nuclear fusion, where Cesium is evaporated in a high temperature flow of dissociated deuterium [2]. Separation effects occur often in rarefied flows due to the different properties of the components of the gas mixture. In atomic mixtures (rare gases, metal vapors, molecular gases dissociated by high temperatures) separation occurs mostly as a consequence of the different atomic mass and momentum transfer cross sections. These phenomena have a large scientific and technological relevance: for example in molecular beam science the separation effect must be taken into account for a correct interpretation of the results [1], while in shock wave/boundary layer problems the atomic separation can affect the heat flow rate on a surface; furthermore, in flows impinging on a catalytic surface it is very important to be able to calculate the composition difference between the free flow and the flow close the surface. Isotopic separation in atomic flows has also been studied [3]. Since these phenomena are essentially a reflex of the flow kinetics, the most appropriate way to describe them is to operate at the kinetic level, by solving kinetic equations.

The direct, deterministic solution of the Boltzmann equation on a grid in phase space [4] could be considered since the small mole fraction of the seed is not a problem for a deterministic method. A discrete ordinate solution of the McCormack form of the Boltzmann equation was actually applied to binary atomic mixtures with comparable mole fractions, in simple geometries and for subsonic flows [5]. These solutions techniques, however, are much difficult to set up for new problems, and the set up is very heavy when complex boundary conditions apply. A stochastic method has usually the advantage of a

* Corresponding author. Address: Dipartimento di Chimica dell'Universita' di Bari, Via Orabona 4, 70126 Bari, Italy.
E-mail address: savino.longo@ba.imip.cnr.it (S. Longo).

0021-9991/$ - see front matter © 2009 Elsevier Inc. All rights reserved.
doi:10.1016/j.jcp.2009.02.016

very simple set up united to reliability and adaptability: the computational cost usually compares to deterministic techniques for high dimensional problems like phase space flows.

The Direct Simulation Monte Carlo Method [6] seems to fit the issue most closely since it is able to treat efficiently multidimensional problems which arise already when considering 2D flows. Unfortunately, DSMC is not the most appropriate technique for this specific problem since it is affected by relatively large numeric diffusion and cannot efficiently treat multi-species problems where some of the species are impurities, and their low concentration requires a high computational cost to reach an acceptable signal to noise ratio. Other methods proposed in the past are to be considered.

Particle/mesh methods, where the velocity distribution function is stored on a grid but propagated by particles [7,8], could also be considered, but the storage problems are not trivial and lead to an unpractical simulation protocol.

Another possibility emerges with the recent reconsideration of stochastic solution of the nonlinear BGK Equations [9–11]: these BGK/MC methods are promising for some applications, but as regards atomic separation the generalization to two components is not trivial and even open to theoretical discussions [12,13]. Furthermore these methods cannot completely solve the numerical diffusion problem, and the use of strongly simplified collision derivatives limits their reliability. Recent improvements, like the introduction of the so-called ellipsoidal target distribution for a BGK equation [14] can only partially alleviate some of the disadvantages of BGK-Monte Carlo methods when they are applied to seeded gas flows, even if they appear promising for many different applications.

The method proposed in this paper for seeded flows is based on the exact Monte Carlo solution of a linear transport equation for each separate component in a flowfield which is preliminarily calculated by a nonlinear Monte Carlo method applied to the main component. The lack of numerical diffusion in the second step allows a reliable evaluation of separation effects. The implementation of the method proposed in a working code is very straightforward and simpler than that of DSMC. The procedure is described here for the first time and applied to a few test cases for illustration and benchmarking.

2. Method of calculation

2.1. General aspects

The method proposed is essentially a Monte Carlo solution [15–17] of a simplified form of the multi-component Boltzmann equation.

The method consists of two stages.

The first stage consists of a fixed time step Monte Carlo solution of the following nonlinear equation:

$$\frac{\partial f_a}{\partial t}+\mathbf{v}\cdot\frac{\partial f_a}{\partial \mathbf{r}}=\int d\Omega d^3 v_1 g\sigma_{aa}(g,\vartheta)\left(f'_a f'_{0a}(f'_a)-f_a f_{0a}(f_a)\right), \tag{1a}$$

where f_a is the unknown translational distribution of the main species, g is the relative speed, $\sigma_{aa}(g,\vartheta)$ is the differential elastic cross section, while f_{0a} is the corresponding local equilibrium distribution based on macroscopic variables, i.e.

$$\begin{aligned} f_{0a} &= n_a(\mathbf{r},t)\left(\frac{m_a}{2\pi k T_a(\mathbf{r},t)}\right)^{3/2}\exp\left(-m_a\frac{(\mathbf{v}-\mathbf{v}_a(\mathbf{r},t))^2}{2kT_a(\mathbf{r},t)}\right),\\ n_a(\mathbf{r},t) &= \int d^3 v f_a,\\ \mathbf{v}_a(\mathbf{r},t) &= n_a^{-1}\int d^3 v \mathbf{v} f_a,\\ kT_a(\mathbf{r},t) &= \frac{1}{3}m_a n_a^{-1}\int d^3 v v^2 f_a-\frac{1}{3}m_a v_a^2. \end{aligned} \tag{1b}$$

This equation is a generalization of the nonlinear BGK equation. It shares with this last the nonlinear character, which allows to describe gas dynamics effects like shock waves, but at the same time the collision term gives a much more detailed description of the local gas kinetics than that provided by a relaxation term.

With respect to the exact collision term, the one used in this study is rewritten in a simplified form where the terms involving the minority species as a target are neglected and the velocity distribution of the majority species is cast into a shifted Maxwell distribution based on the local and instantaneous density, mean velocity and static temperature of this species as sampled on a numerical mesh. The macroscopic quantities necessary to generate the target distribution are sampled on a space grid.

The first approximation applies if the mole fractions of the impurity components are much smaller than one, which is usually the case for seeded flows. It is also trivially exact when the main component is considered as a seed, a case also functional to our method.

As concerns the second approximation, it corresponds to a first order Chapman–Enskog expansion since the product term in the Boltzmann collision term can be approximated as shown in the following Eq. (1) neglecting a term which is second order in the expansion. This approximation leads therefore to the Navier–Stokes equations in the continuum limit. At the same time, the use of a phase space characteristic method allows a robust treatment of rarefied regions eventually present in the domain.

In the second step, an exact, stochastic solution method is applied to the linear equation:

$$\frac{\partial f_i}{\partial t} + \mathbf{v} \cdot \frac{\partial f_i}{\partial \mathbf{r}} = \int d\Omega d^3 \, v_1 g \sigma_{ia}(g, \vartheta)(f_i' f_{0a}' - f_i f_{0a}), \tag{2}$$

where f_i is the translational distribution of the ith component, including the main one, while f_{0a} is the local equilibrium distribution obtained from the solution of Eqs. (1a) and (1b) in the first step and σ_{ia} is the differential cross section for the elastic scattering between the ith and the main species. This amounts to solve the equations for the main component twice, the first time approximately as a bulk species and the second time as if it were another impurity.

2.2. Nonlinear bulk kinetics

The solution of Eqs. (1a) and (1b) is obtained by using a nonlinear, self-consistent version of test particle Monte Carlo (TPMC) method of Ref. [15], where $f_{0a}(\mathbf{r},\mathbf{v})$ is not given but determined from the simulation. The particle handling and storage is much closer to BGK/MC [10–12] methods than to DSMC, therefore much simpler, while the collision treatment is close to that used in thermal neutron or ion transport and based on the sampling of a "virtual" target particle from a local equilibrium distribution.

During a time step the following operations are performed.

(I) First, particles are moved according to their velocity:

$$\mathbf{r}(t + \Delta t) = \mathbf{r}(t) + \mathbf{v}(t)\Delta t. \tag{3}$$

The velocity vectors $\mathbf{v}(t)$ are always three dimensional, in order to match the exact specific heat ratio γ (=5/3 for atoms). For simplicity it is possible to use a fixed number of particles, which are injected back from the inlet when they leave the simulation domain. Solid obstacles (diagnostic devices, reactor walls) are included in the model by mapping the mesh onto a logical matrix. Solid-filled mesh elements are easily detected during the particle motion. Adiabatic isotropic diffusion is simply implemented by replacing the particle into the previous position and selecting a random rotation of the particle velocity until the advance step ends outside the solid. The solid surface model can easily be extended to describe partial or total thermal equilibration of the particles with the surface, when appropriate.

(II) Second, particles contribute to the local averages based on the formulas

$$\langle n(\mathbf{r}, t)\rangle_c = \frac{w}{V_c}\sum_p S_c(\mathbf{r}_p), \langle a\rangle_c = \frac{\sum_p S_c(\mathbf{r}_p) a_p}{\sum_p S_c(\mathbf{r}_p)}, \tag{4}$$

where c is the cell index, p is the particle index, $S_c(\mathbf{r})$ is the characteristic function of c-th cell, a_p is a single particle quantity (e.g. v_p^2), $n(\mathbf{r}, t)$ is the local number density at the time t, V_c is the cell volume. The real to simulated particle ratio w is fixed in order to fit the requested physical conditions.

(III) For every particle a virtual target particle with vector velocity $\mathbf{v}_1$ is generated. The collision probability with the test particle moving with the velocity $\mathbf{v}$ is given by

$$p_{\mathbf{vv}_1} = 1 - \exp(-g\sigma(g)n(\mathbf{r}, t)\Delta t), \tag{5}$$

where σ is the diffusion cross section and $g = |\mathbf{v} - \mathbf{v}_1|$is the relative speed. The target particle velocity $\mathbf{v}_1$ is a stochastic variable distributed according to the distribution $f_{0a}(\mathbf{r}, \mathbf{v}_1, t)$ and can be produced by the following formula applied to each velocity component:

$$v_{1i} = h(2/3)^{1/2}\sqrt{\left\langle (\mathbf{v} - \langle \mathbf{v}\rangle)^2 \right\rangle} + \langle v_i\rangle, \tag{6}$$

where the averages denoted by $< \cdots >$ are calculated in the previous step, the index $i = 1, 2, 3$ specifies the Cartesian component and h is a random number extracted from an ensemble with a $\exp(-h^2)$ distribution. This last ensemble is conveniently generated by the von Neumann rejection method and stored in a vector variable to increase the calculation speed.If the collision occurs, i.e. $\eta < p_{\mathbf{vv}_1}$ where η is a random number from a uniform distribution, $0 < \eta \leqslant 1$, then a new relative velocity $\mathbf{g}'$ is produced as a random vector sampled from an appropriate distribution (for most cases an isotropic distribution is appropriate if the cross section used is the momentum transfer one) and the new particle velocity $\mathbf{v}'$ is calculated as

$$\mathbf{v}' = \frac{m\mathbf{v} + m_1\mathbf{v}_1}{m + m_1} + \frac{m_1}{m + m_1}\mathbf{g}'. \tag{7}$$

(IV) Energy and momentum conservation is enforced. To this aim a new sampling to the grid is performed without canceling results of the previous one. Then the particle velocities are scaled in any cell in order to match the previous sampling results by using the following procedure which is applied only to particles not alone in their cell:

$$\mathbf{v} \leftarrow (\mathbf{v} - \mathbf{a}')\sqrt{\frac{b}{b'}} + \mathbf{a}, \tag{8}$$

where $\mathbf{a} = \langle \mathbf{v} \rangle$, $\mathbf{a}' = \langle \mathbf{v}' \rangle$, $b = \langle \mathbf{v}^2 \rangle - a^2$, $b' = \langle \mathbf{v}'^2 \rangle - a'^2$, the superscript refers to the post collision sampling results, and the averages are on the mesh cell.

It must be noted that in the application of this procedure any particle communicates only with the cell and not with other particles directly, therefore it is not necessary to build a dynamic list of particles present in any cell like in DSMC.

Calculations based on the iteration of a cycle composed by the procedures (I)–(IV) are run until a steady state condition is reached. After the steady state is reached the space resolved number density, temperature and velocity components of the main species are calculated and cast into vectors for the separation calculations described in the next section.

2.3. Multi-component linear refinement

The final determination of both the main component and the impurity components related quantities is based on a TPMC technique analogous to those used for thermal neutron transport [16,17] but where the particle-thermal background collision term is sampled as in [15] (where a formal proof that Eq. (2) is solved exactly by this procedure in found in Appendix 2).

In short, the transport equation is rewritten in an integral form and its solution is expanded as a convergent Neumann series. The terms in the series are shown to be estimated systematically and exactly using suitably chosen stochastic processes. These processes can be interpreted as particle trajectories. The demonstration is fully general under the only hypothesis that the transport equation is linear.

This calculation step is totally free of numerical diffusion since no information is propagated by the grid, which is only used to detect obstacles and to store values of the quantities calculated in the previous stage and their functions.

The ith component undergoes collisions with main species particles with a frequency preliminary estimated as:

$$\nu_i(\mathbf{r}) = C \cdot n(\mathbf{r}) \sigma_i(kT(\mathbf{r})) \sqrt{\frac{kT(\mathbf{r})}{\pi \mu_i}}, \tag{9}$$

where $n(\mathbf{r})$, $T(\mathbf{r})$ are respectively, the local number density and temperature of the target species, $\sigma(kT(\mathbf{r}))$ the temperature corrected average cross section for the process (for rigid spheres this is a constant) and $\mu_i = m_i m_a/(m_i + m_a)$ is the reduced mass. A suitable global value for the proportionality constant C, which is usually about 10, is selected following the rule described later in this section. The real collision frequency, taking into account the thermal velocity distribution of target particles, is matched by removing excess collisions (null collisions) using appropriate collision probabilities (see below). The time to next collision t_c (different for all particles) is calculated by the usual relation

$$t_c = -(1/\nu_i(\mathbf{r})) \ln \eta, \tag{10}$$

where η is a random number from a uniform distribution, $0 < \eta \leqslant 1$. Particles are moved for the stochastic time t_c, whose value is different for all flights and for all particles, using Eq. (3) and the same treatment of boundary conditions as in Section 2.2.

After any free flight the candidate collision partner, a main component atom, is sampled as in the previous section. The collision probability is given this time by:

$$p_{\mathbf{vv}_1} = \frac{n(\mathbf{r}) \sigma_i(g) g}{\nu_i(\mathbf{r})}. \tag{11}$$

Again, sampled a random number $0 < \eta < 1$ from a uniform distribution, the collision occurs if $\eta < p_{\mathbf{vv}_1}$. If the collision occurs the post collision velocity is calculated using Eq. (7).

Of course $p_{\mathbf{vv}_1}$ must be always <1 in view of its physical meaning. The use of local maximization of the collision frequency given by Eq. (9) allows a strong reduction of the computational cost and is verified a posteriori by checking that the fraction of computed collisions with $p_{\mathbf{vv}_1} > 1$ is insignificant, e.g. $<10^{-3}$. Otherwise, C needs to be increased until the condition is satisfied.

For the case of the main component, the differences between the flow field preliminarily calculated through the nonlinear equation and the linear refinement provide an estimate of the precision of the approximations made in the first step. This method can be used to evaluate the precision of other kinds of flow calculations.

3. Examples

In this section, three cases are considered to illustrate the method. In all cases a transonic flow of He is considered with Ar as impurity component. The corresponding mass ratio of about 10 is rather high and leads to distinct separation phenomena. For a first evaluation of the proposed technique, rigid sphere scattering is assumed with the momentum transfer total cross sections for He/He and He/Ar reported in Ref. [18]. This solution has been also selected for a simpler comparison of test case results with those obtained by using other models in the next future. Of course for technical applications the VSS cross section [6] or even better cross sections based on quantum calculations are to be preferred. In Ref. [19] the reader can find a comparison between results obtained using different cross sections in an expanding atomic beam based on a preliminary

version of the code presented in this work. In these examples, Δt equals $0.1d/v_{th}$, where d is the grid spacing and v_{th} is the thermal speed in the free flow.

The first two test cases are paradigmatic and involve a flow around a cylindrical obstacle. The surface of the cylinder is an adiabatic diffuser.

In the unperturbed free flow the Mach number is $M = 3$ and the Knudsen number is $Kn_\infty = 0.5$ and 0.05 respectively ($Kn_\infty = \lambda_\infty/R$).

The w coefficient of Eq. (4) is fixed by the following formula valid for a supersonic injection with $M \geqslant 3$ and based on the equivalence of numerical and physical particle fluxes:

$$w = n_0 M \sqrt{\gamma k T_0/m}/\Phi_p, \tag{12}$$

where Φ_p is the flux of injected numerical particles, evaluated in the course of the simulation by a time average and $\gamma = 5/3$ is the specific heat ratio. The simulation domain is actually larger than those shown in the following Fig. 1: the real height is about three times the portion shown, in order to avoid interactions of the upper side with the shock. The grid for the full domain is uniform with 200×150 cells. The number of simulated particles is 3×10^5 in both the first and second stage. In the first stage 4000 time steps are needed to reach the steady state and the dynamic quantities are collected for further 4000 time steps. In the second stage, a total of 1.3×10^9 events is sampled.

The results for these test cases are reported in Fig. 1. Those for the density of the main component (He) are close to those reported in Ref. [4] and obtained by deterministic numerical solution of the Boltzmann equation for an atomic gas with adaptive grid equation and in the same conditions. In particular, for the less rarefied case where it is possible to check out the shock front contour and the standoff distance, results for these two methods agree closely as well as the somewhat elusive W-shaped structure in the wake region, which is produced by both models. Let us illustrate the separation of Ar and He. As expected, separation effects are more relevant in the higher Kn case. In both cases however the flow is impoverished of the more massive impurity (Ar) entering the shock front, and it is enriched just after the shock. This effect is essentially due to the fact that momentum relaxation of a higher mass impurity is slower than that in the main gas: therefore Ar atoms move faster in the shock than He ones and consequently their relative density decreases because of mass conservation. Another separation region is observed in the wake, which is impoverished in Ar. This last effect can be explained by the different thermal speed of the two particle species: He is faster in filling a vacuum.

The third case is an internal supersonic flow in a channel, which is partially obstructed by a transversal rigid plate. This problem is similar to the classic step one but includes a wake region, which makes it more challenging. Furthermore, by symmetry this test case can represent the effect of a grid, which is frequent in applications. The channel walls are reflective diffusers (otherwise a boundary layer would appear) while the obstacle surfaces are adiabatic diffusers.

In the unperturbed free flow the gas temperature is 219 K, the Mach number is $M = 5$ and the gas density is $n_0 = 4.5 \times 10^{21}$ m^{-3}corresponding to $Kn \cong 0.1$.

2×10^5 particles are simulated in the first stage for 4000 time steps to reach a steady state and the results are averaged over 4000 additional time steps to reduce the statistical noise. The grid is uniform with 100×100 cells. In the second stage, a total of 1.7×10^8 events is sampled.

In Fig. 2a–c the number density, static temperature and Mach number of the main species are plotted: as can be seen while the Knudsen number is quite high, a wide primary shock is observed and only a remnant of the features of the interaction between direct and reflected shock is observed on the right of the picture. This test case also displays a rarefaction wake after the obstacle and a boundary layer on its front surface, and globally it is representative of diffuse technological test cases where a seeded supersonic gas flow impinges on a structure placed in a vacuum chamber. Very small deviations are observed in this case between the preliminary and refined determination of the main specie flow, weakly affecting the shock profile just in front of the obstacle and the expansion region in the wake. We now come to the seed component quantities. Fig. 2d shows the ratio of the Ar fraction to that at the inlet, to show more directly the separation effect.

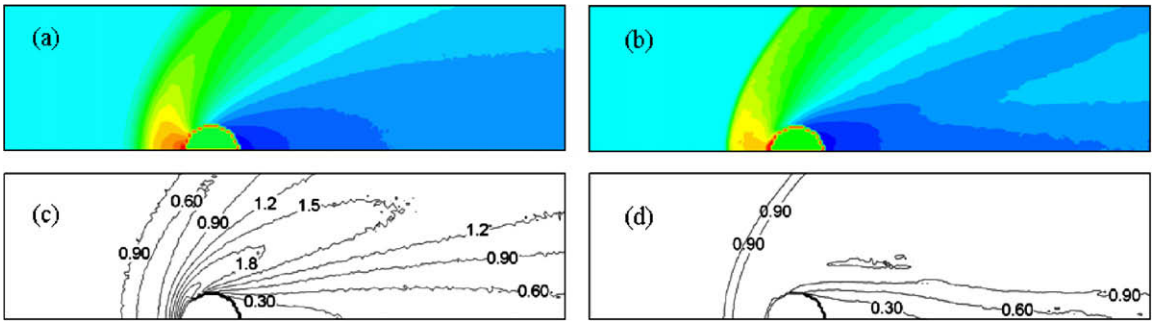

Fig. 1. Results for a supersonic flow ($M = 3$) of He seeded with Ar, on a cylinder. Left (a,c): $Kn = 0.5$; Right (b,d): $Kn = 0.05$. Top (a,b): density profile of He. Bottom (c,d): ratio of the mole fraction of Ar to the free flow one.

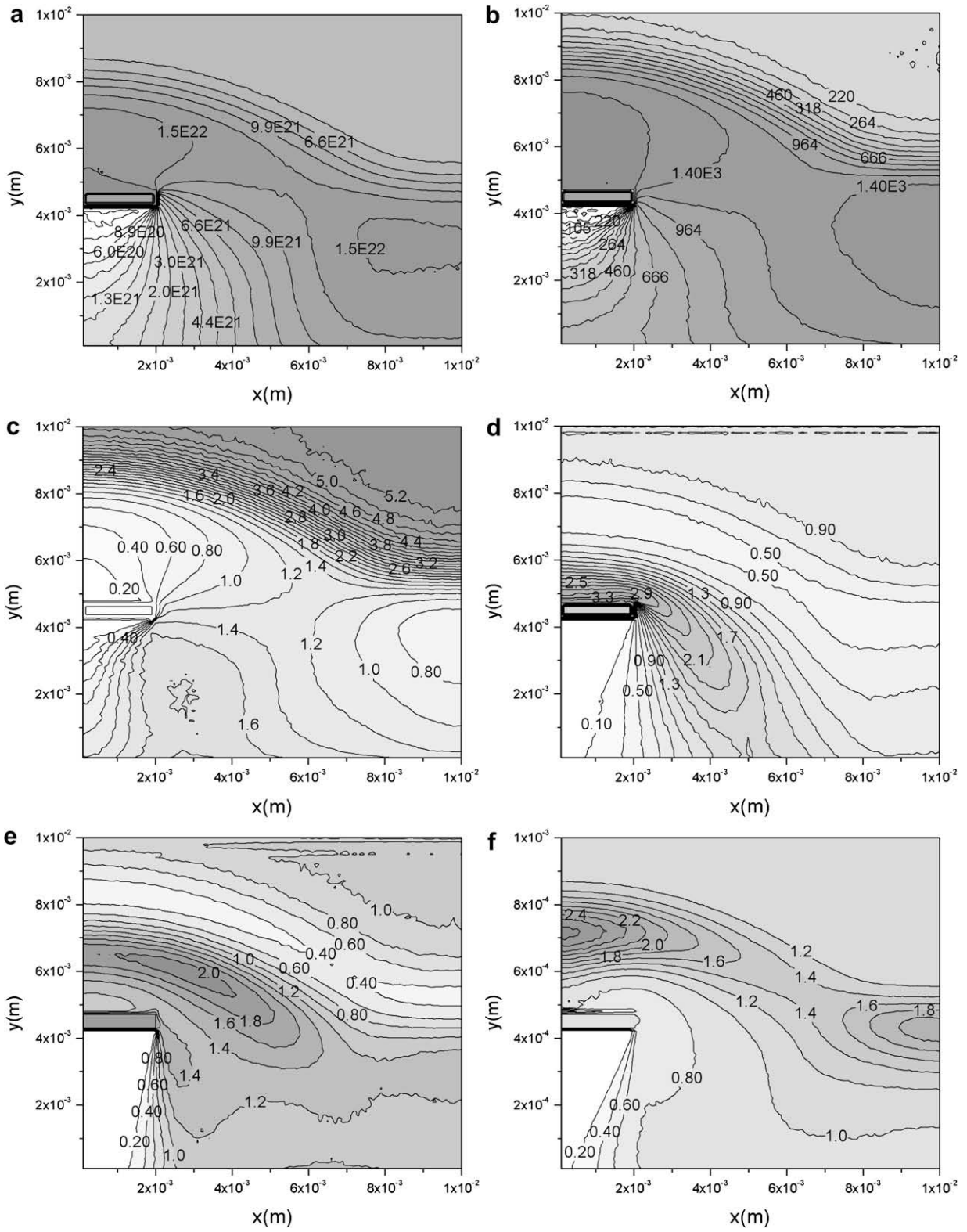

Fig. 2. (a) Main species (He) number density (m^{-3}), (b) main species (He) temperature (K), (c) main species (He) Mach number, (d) ratio of the mole fraction of Ar to that at the inlet, (e) ratio of the impurity to the main species temperature, (f) ratio of the impurity to the main species speed, for a $M = 5$ flow in a partially obstructed channel, $Kn = 0.1$ (evaluated with respect to the channel width). In this picture, the flow enters from the upper side.

At this low pressure the features of separation effects are well visible: the flow is strongly impoverished of the more massive impurity when entering any shock front, and it is enriched just after the shock and specially in the boundary layer on the front side of the obstacle. Again another separation region is observed in the wake.

The behavior of static temperatures is also understandable, assuming that the thermal relaxation of the massive impurity is delayed with respect to that of the bulk gas Fig. 2e. The delay is essentially due to the fact that the inter-component heat transfer rate is proportional to the small parameter m/M [20] where in this case m is the He atom mass and M is the Ar one. In Fig. 2f, a similar effect produces a non-null average relative speed of the two components (velocity slip): this feature is easily masked by statistical fluctuation and numerical effects, but our procedure is able to evaluate its amount with ease and with a modest computational cost. Well detectable are the deceleration slip in the primary and reflected shocks, and the acceleration slip in the wake region.

All these runs were executed on a computer with a 2.4 GHz Intel Core Duo processor.

Let us discuss briefly the computational cost of the results. The results in Fig. 1 required about 100′, most of which devoted to the exact solution of the linear problem in both cases. The results in Fig. 2 required about 40′ minutes shared almost equally between the two stages.

The computational cost is not much variable with Kn. This can be understood since much of the computational time is spent after the steady state is reached, in order to collect a satisfactory statistics. Under such conditions, the computational cost is determined by the desired relative variance and is controlled by changing the number of particles and sampling steps.

In this context, the use of linear transport methods well developed for thermal neutrons offers the possibility to borrow standard variance reduction techniques from this field [16,17]. For example, if an estimate of the separation effect is needed in the shock front, it is possible to inject particles in the flow just before the shock and remove them just after it. In this way a drastic reduction of the computational cost is possible. A more advanced treatment can employ the adjoint equation in order to provide local solutions for a few space positions of interest.

4. Conclusions

A practical method is proposed for the calculation of seeded atomic flows in the transition regime. The basic idea is that the nonlinear fluid dynamics of the main component is treated first, while the final determination of all components is made by using the linear test particle Monte Carlo method which is totally free of numerical diffusion being based on the accurate implementation of the free flight time (or length). The method proposed is actually of simpler implementation than DSMC recipes in spite of its obvious advantages for the treatment of seeded atomic flows, namely the variance reduction in the treatment of the impurities and the expected good reliability of the calculated atomic separation in view of the lack of numerical diffusion. The transport of more complex and structured seed species (e.g. molecules) should be possible by straightforward extensions of the linear part of the model.

Acknowledgement

This work was partially supported by “Fondi di Ateneo Uniba (60%) 2007”

References

[1] G. Sanna, G. Tomassetti, Molecular Beams Gas Dynamics, Imperial College Press, London, 2005.
[2] J. Peters, Negative ion sources for high energy accelerators, Rev. Sci. Instr. 71 (2000) 1069.
[3] R. Chiba, E. Kakuya, K. Kaneko, Isotope separation of argon by axial flow turbo-machine (I) separation effect for molecular flow, J. Nucl. Sci. Technol. 14 (7) (1977) 502–505.
[4] V.I. Kolobov, R.R. Arslanbekov, V.V. Aristov, A.A. Frolova, S.A. Zabelok, Unified solver for rarefied and continuum flows with adaptive mesh and algorithm refinement, J. Comput. Phys. 223 (2007) 589–608.
[5] S. Naris, D. Valougeorgis, D. Kalempa, F. Sharipov, Gaseous mixture flow between two parallel plates in the whole range of the gas rarefaction, Physica A 336 (2004) 294.
[6] G.A. Bird, Molecular Gas Dynamics and the Direct Simulation of Gas Flows, Oxford Univ. Press, 1994.
[7] J.K. Haviland, M.L. Lavin, Application of the Monte Carlo method to heat transfer in a rarefied gas, Phys. Fluids 5 (1962) 1399.
[8] S. Longo, I.D. Boyd, Implementation of a self-consistent Monte Carlo method to solve the nonlinear Boltzmann equation, in: Proceedings of the 21st International Symposium on Rarefied Gas Dynamics, Cépaduès ed., vol. II, Toulouse, France, 1999, pp. 47–54.
[9] M. Lee, J.W. Dufty, J.M. Montanero, A. Santos, J.F. Lutsko, Long wavelength instability for uniform shear flow, Phys. Rev. Lett. 76 (1996) 2702–2705.
[10] M.N. Macrossan, A particle simulation method for the BGK equation, in: Proceedings of the 22nd International Symposium on Rarefied Gas Dynamics, AIP Conference Proceedings, vol. 585, 2001, p. 426.
[11] D. Bruno, S. Longo, Monte Carlo simulation of nearly kinematic shock fronts in rarefied gases, Eur. Phys. J. Appl. Phys. 17 (2002) 233–241.
[12] D. Bruno, S. Longo, M. Capitelli, A BGK/MC Method for the Simulation of Shock Waves in Binary Mixtures, AIAA 2002-2895.
[13] P. Andries, K. Aoki, B. Perthame, A consistent BGK-type model for gas mixtures, J. Stat. Phys. 106 (2002) 993.
[14] J.M. Burt, I.D. Boyd, Evaluation of a Particle Method for the Ellipsoidal Statistical Bhatnagar–Gross–Krook Equation, AIAA-2006-0989.
[15] S. Longo, P. Diomede, Monte Carlo modeling of gas phase ion transport under thermal gradients and external fields, Eur. Phys. J. Appl. Phys. 26 (2004) 177–185.
[16] J. Spanier, E.M. Gelbard, Monte Carlo Principles and Neutron Transport Problems, Addison Wesley, 1969 (Chapter 5, reprinted Dover 2008).
[17] S.A. Dupree, S.K. Fraley, A Monte Carlo primer: practical approach to radiation transport, Kluwer, 2002.
[18] M.A. Lieberman, A.J. Lichtenberg, Principles of Plasma Discharges and Material Processing, Wiley, 2005.
[19] S. Longo, P. Diomede, A. Laricchiuta, G. Colonna, M. Capitelli, D. Ascenzi, M. Scotoni, P. Tosi, F. Pirani, From microscopic to macroscopic modeling of supersonic seeded atomic beam, Lect. Notes Comp. Sci. 5072 (2008) 1131–1140.
[20] E.M. Lifshitz, L.P. Pitaefskij, Physical Kinetics §12 and §42, Pergamon Press, 1981.